# Synthesis, Characterization, Photo-Induced Alignment, and Surface Orientation of Poly(9,9-dioctylfluorene-*alt*-azobenzene)s

**Kenji Kinashi,[1] Yuki Kambe,[2] Masahiro Misaki,[2] Yasuko Koshiba,[2] Kenji Ishida,[2] Yasukiyo Ueda[2]**

[1]Department of Macromolecular Science and Engineering, Kyoto Institute of Technology, Matsugasaki, Sakyo, Kyoto 606-8585, Japan
[2]Department of Chemical Science and Engineering, Graduate School of Engineering, Kobe University, Rokko, Nada, Kobe 657-8501, Japan
Correspondence to: Y. Ueda (E-mail: yueda@kobe-u.ac.jp)

Received 8 June 2012; accepted 12 August 2012; published online
**DOI: 10.1002/pola.26338**

**ABSTRACT**: Three types of bi-functionalized copolymers (**P1FAz**, **P2FAz**, and **P3FAz**) with different numbers of fluorene units and an azobenzene unit were synthesized and characterized using UV–vis and polarized absorption spectroanalysis. The *trans-cis* photoisomerization was conformed under 400 nm light irradiation for all copolymers in chloroform. However, in the film state, only the *trans-cis* photoisomerization occurred by mono-fluorene attached copolymer poly[(9,9-di-*n*-octylfluorenyl-2,7-diyl)-*alt*-4,4′-azobenzene)] (**P1FAz**). Photo-induced alignment was achieved using the **P1FAz** film after irradiation with linear polarized 400 nm light and subsequent annealing at 60 °C. Surface orientation of a spin-coating film of poly(9,9-didodecylfluorene) (**F12**) was achieved using the photo-induced alignment layer of the **P1FAz** film after annealing at 90 °C. The photo-induced alignment layer of **P1FAz** has potential application to the surface orientation technique for appropriate polymers, which will be useful for the fabrication of optoelectronics devices. © 2012 Wiley Periodicals, Inc. J Polym Sci Part A: Polym Chem 000: 000–000, 2012

**KEYWORDS**: azo polymers; functionalization of polymers; orientation; photochemistry; synthesis

**INTRODUCTION** The static and dynamic properties of liquid crystals are strongly affected by the nature of the film surface alignment. Mechanically rubbed polyimide films have been commercially used as alignment films for liquid crystal molecules.[1,2] However, the rubbing process of alignment induces several defects, such as electrostatic charges or dust generation. Therefore, the photo-induced alignment technique has received considerable attention as a rubbing-free and pattern-able process.[3] The photo-induced alignment of liquid crystals with the use of photosensitive materials based on *trans*-to-*cis* photoisomerization,[4–8] photocrosslinking involving photodimerization,[9–11] and photodissociation[12] has been reported. Some of the photo-induced alignment materials exhibit reversible liquid crystal alignment regulation. For example, a functional polymer based on a photochromic compound can reversibly control liquid crystal alignment triggered by *trans-cis* photoisomerization. Therefore, photo-induced alignment based on *trans-cis* photoisomerization by irradiation with linear polarized light is one of the most attractive candidate techniques for surface control, which can archive a surface orientation with respect to the next upper layer. Azobenzenes are well-known as photosensitive chromophores that undergo *trans-cis* photoisomerization upon irradiation with light of an appropriate wavelength in a solution or in an appropriate host matrix.[13–16] Repetition of such photoisomerization in a host matrix leads to perpendicular alignment of the long axis of the azobenzene chromophore to the electric field vector of the linear polarized light, which eventually induces anisotropy. Therefore, azobenzene-functionalized polymers have attracted considerable attention with anisotropy induced by linear polarized light irradiation below the glass-transition temperature.[17,18] Poly(9,9-dioctylfluorene) is a polymer that forms good alignment layers that exhibit a high dichroic ratio at an absorbance of ∼10 using a friction-transfer technique and subsequent annealing below the glass-transition temperature.[19] Furthermore, a highly orientated 9,9-dioctylfluorene film has been used to successfully fabricate highly polarized light-emitting diodes.[20] Thus, a bi-functionalized copolymer based on 9,9-dioctylfluorene and azobenzene moieties would have performance advantages with a significant promise for surface orientation.

In this article, we report the synthesis and photochemical characteristics of three different poly(9,9-dioctylfluorene-*alt*-

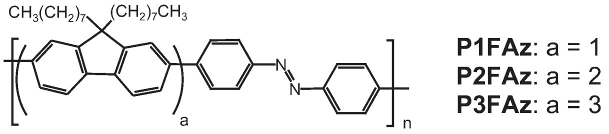

**FIGURE 1** Chemical structure of poly(9,9-dioctylfluorene) copolymers.

azobenzene) copolymers (Fig. 1) and their potential for use as alignment layers.

## EXPERIMENTAL

The chemical structures of the synthesized compounds were characterized by $^1$H nuclear magnetic spectroscopy (NMR; Bruker Advance500), $CDCl_3$ solvent, tetramethylsilane (internal standard), and time-of-flight mass spectrometry (PerSeptive Biosystems Mariner). Melting points (mp) were determined using a melting point apparatus (Yanaco MP-500P) with a digital thermometer. UV–vis absorption and photoluminescence (PL) spectra were recorded on Jasco V-670 and Hitachi F-2500 spectrophotometers, respectively. The relative fluorescence quantum yields ($\Phi_f$) were measured using a PL spectrophotometer (Hitachi F-2500, anthracene or pyrene in ethanol as common standards). The morphologies of the films were characterized by atomic force microscopy (AFM; Seiko Instruments SPI-3700). The photoisomer was obtained by irradiation with light from a Xe lamp (Asahi spectra MAX-301, 300 W) passed through a 400 nm band pass filter. The irradiation intensity was 20 mW cm$^{-2}$. The light from a Xe lamp was passed through a band pass filter and a polarizing to produce a parallel beam of linear polarized light with a wavelength in the vicinity of 400 nm (10 J cm$^{-2}$). Absorption and PL spectral measurements were performed in chloroform using in a quartz cell with a path length of 1 cm. Films were spin-coated from 0.025 wt % chloroform solutions onto a fused silica substrate at 1500 rpm for 30 s.

## SYNTHESIS

### 4,4′-Diiodoazobenzene (1)

A solution of KOH (3.7 g, 66 mmol) in methanol was slowly added to a solution of aluminum powder (0.51 g, 18.8 mmol) and 4-iodonitrobenzene (2.45 g, 9.8 mmol) in methanol (6 mL), and the mixture was refluxed by stirring for 4 h under an argon atmosphere. The reaction mixture was cooled to room temperature and the precipitated crude product was separated by filtration, as well as then washed with dichloromethane and dilute hydrochloric acid to maintain the pH at 4. The filtered solution was extracted with water, and the organic layer was dried over anhydrous $MgSO_4$ and concentrated *in vacuo*. The crude product was sublimed onto a cold finger to give **1** as orange plate-like crystals (0.72 g, 1.66 mmol, 17%).

mp: 236–240 °C. $R_f$: 0.9 (for chloroform). ATR-FTIR (cm$^{-1}$): 1573, 1558, 1468, 1392, 1296, 1096, 1049, 1000, 832, 713. DI-MS: *m/z* 433 [M+]. $^1$H NMR (500 MHz, $CDCl_3$): $\delta$ (ppm) 7.64 (d, 4H, $J = 8.5$ Hz), 7.86 (d, 4H, $J = 8.5$ Hz).

### Poly[(9,9-di-*n*-octylfluorenyl-2,7-diyl)-*alt*-4,4′-azobenzene)] (P1FAz)

Compound **1** (80 mg, 0.19 mmol), 9,9-dioctylfluorene-2,7-diboronic acid bis(1,3-propanediol)ester (100 mg, 0.18 mmol), and $(PPh_3)_4Pd(0)$ (2 mg) were dissolved in a mixture of toluene (3 mL) and $K_2CO_3$ (2 M, 1.8 mL) under an argon atmosphere. The solution was maintained at 70 °C with vigorous stirring for 45 h and then poured into a large amount of cold methanol. The precipitated crude product was separated twice by filtration to remove oligomers and catalysts residues. The polymer was obtained as a yellow solid (93 mg, 0.17 mmol, 94%).

mp: decomposed at 292 °C. $M_w$: 17,000 g mol$^{-1}$, $M_w/M_n = 1.7$. ATR-FTIR (cm$^{-1}$): 2924, 2851, 1598, 1464, 1406, 1340, 1158, 1010, 854, 819, 745.

### 2-Bromo-9,9-di-*n*-octylfluorene (2)

1-Octylbromide (3.5 g, 18.0 mmol) were slowly added to a suspension containing 2-bromofluorene (2.0 g, 8.2 mmol), benzyltriethylammonium chloride (96 mg, 0.42 mmol), aqueous NaOH solution (3.5 mL, 50 wt %), and sieve-dried dimethyl sulfoxide (DMSO; 16 mL). The mixture was vigorously stirred at 35 °C for 7.5 h and then extracted with diethyl ether. The organic layer was washed with water, dilute hydrochloric acid, and brine, and the resulting organic layer was dried over anhydrous $MgSO_4$ and concentrated *in vacuo*. The resulting crude red oil was purified by column chromatography using hexane as an eluent to give **2** as a pale yellow oil (3.1 g, 6.6 mmol, 80%). $R_f$: 0.7 (for hexane).

$^1$H NMR (500 MHz, $CDCl_3$): $\delta$ (ppm) 7.65 (m, 1H), 7.54 (d, 2H), 7.43 (m, 2H), 7.32 (m, 3H), 1.95–1.84 (m, 4H), 1.45–1.04 (m, 20H), 0.88–0.80 (m, 6H), 0.60–0.58 (m, 4H).

### 9,9,9′,9′-Tetra-*n*-octyl-2,2′-bifluorene (3)

*n*-Butyllithium (*n*-BuLi) in hexane (1.6 M, 2.2 mL) was added slowly to a solution of **2** (1.5 g, 3.3 mmol) in tetrahydrofuran (THF; 10 mL) at −78 °C under an argon atmosphere and stirred for 1 h. Trimethyl borate (1 mL) was added to the mixture at −78 °C, which was then warmed slowly to room temperature with continuous stirring for 5 h. The mixture was then cooled slowly to 0 °C, and dilute hydrochloric acid (3 mL) was added to the mixture. The mixture was extracted with diethyl ether and the resulting organic layer was dried over anhydrous $MgSO_4$. Concentration *in vacuo* gave the corresponding 9,9-di-*n*-octylfluorene-2-boronic acid, which without further purification due to instability, was mixed with **2** (1.5 g, 3.3 mmol) in toluene (10 mL) under a nitrogen atmosphere. The mixture was then added to a solution of aqueous $K_2CO_3$ (2.0 M, 5 mL) and $Pd(PPh_3)_4(0)$ (13 mg), which was stirred under reflux at 75 °C for 40 h. The mixture was extracted with diethyl ether and washed with dilute hydrochloric acid, and the resulting organic layer was dried over anhydrous $MgSO_4$ and concentrated *in vacuo*. The crude product was purified by column chromatography using hexane/dichloromethane (10/1) as an eluent to give **3** as a pale blue oil (1.0 g, 1.3 mmol, 39%). $R_f$: 0.2 (for hexane).

$^1$H NMR (500 MHz, $CDCl_3$): $\delta$ (ppm) 7.76 (d, 2H, $J = 7.5$ Hz), 7.73 (d, 2H, $J = 7.5$ Hz), 7.65–7.61 (m, 4H), 7.37–7.31 (m, 6H), 2.04–2.00 (m, 8H), 1.27–1.07 (m, 40H), 0.80 (t, 12H), 0.72–0.70 (m, 8H).

### 7,7′-Dibromo-9,9,9′,9′-tetra-*n*-octyl-2,2′-bifluorene (4)

A solution of **3** (1.0 g, 1.3 mmol) in dichloromethane (1 mL) was added to a solution of bromine (1.0 g, 6.3 mmol) in dichloromethane (3 mL), and the mixture was refluxed with stirring for 1.5 h under an argon atmosphere. The mixture was poured into water and washed with sodium thiosulfate until the red color disappeared. The combined organic layer was dried over anhydrous $MgSO_4$ and concentrated *in vacuo* to give **4** as a pale yellow oil (1.2 g, 1.3 mmol, ca. 100%). $R_f$: 0.8 (for hexane).

$^1$H NMR (500 MHz, $CDCl_3$): $\delta$ (ppm) 7.57–7.43 (m, 12H), 2.04–1.89 (m, 8H), 1.26–1.07 (m, 40H), 0.83 (t, 12H), 0.69–0.61 (m, 8H).

### Poly[(9,9,9′,9′-tetra-*n*-octylfluorenyl-2,7′-diyl)-*alt*-4,4′-azobenzene)] (P2FAz)

*n*-BuLi in hexane (1.6 M, 2.2 mL) was added slowly to a stirred solution of **4** (0.2 g, 0.5 mmol) in THF (10 mL) at −78 °C under an argon atmosphere, and the mixture was stirred for 1 h. Trimethyl borate (9 mL) was slowly added at −78 °C, and the mixture was then warmed slowly to room temperature and stirred continuously for 10 h. The mixture was slowly cooled to 0 °C and then dilute hydrochloric acid (6 mL) was added. The mixture was extracted with diethyl ether and the resulting organic layer was dried over anhydrous $MgSO_4$. Concentration *in vacuo* gave the corresponding 9,9,9′,9′-tetra-*n*-octyl-7,7′-bifluorene-2,2′-diboronic acid, which without further purification due to instability, was mixed with **1** (0.2 g, 0.5 mmol) in toluene (10 mL) under a nitrogen atmosphere. The mixture was then added to a solution of aqueous $K_2CO_3$ (2.0 M, 1.8 mL) and $Pd(PPh_3)_4(0)$ (6 mg) and stirred under reflux at 70 °C for 45 h. The mixture was extracted with diethyl ether and washed with dilute hydrochloric acid, and the resulting organic layer was dried over anhydrous $MgSO_4$ and concentrated *in vacuo*. The crude product was filtrated and washed with toluene to give **PF2Az** as an orange powder (135 mg, 0.15 mmol, 30%).

mp: 133–150 °C, decomposed at 235 °C. $M_w$: 7300 g mol$^{-1}$, $M_w/M_n = 1.8$. $^1$H NMR (500 MHz, $CDCl_3$): $\delta$ (ppm) 8.10–8.05 (br), 7.88–7.83 (br), 7.71–7.67 (br), 2.17–2.05 (br), 1.12 (br), 0.80 (br). ATR-FT-IR (cm$^{-1}$): 2924, 2852, 1598, 1462, 1157, 1168, 1004, 850, 821, 741.

### 9,9,9′,9′,9″,9″-Hexa-*n*-octyl-2,2′,7′,2″-terfluorene (5)

Compound **2** (1.3 g, 2.9 mmol), 9,9-dioctylfluorene-2,7-diboronic acid bis(1,3-propanediol)ester (0.8 g, 1.4 mmol), and $(PPh_3)_4Pd(0)$ (16 mg) were dissolved in a mixture of toluene (10 mL) and $K_2CO_3$ (2 M, 6 mL) under an argon atmosphere. The solution was maintained at 70 °C with vigorous stirring for 24 h. The mixture was then extracted with diethyl ether and washed with dilute hydrochloric acid, and the resulting organic layer was dried over anhydrous $MgSO_4$ and concentrated *in vacuo*. The crude product was purified by column chromatography using hexane/dichloromethane (10/1) as an eluent to give **5** as a pale blue oil (0.7 g, 0.6 mmol, 43%). $R_f$: 0.3 (for hexane/dichloromethane 10/1).

$^1$H NMR (500 MHz, $CDCl_3$): $\delta$ (ppm) 7.82–7.62 (m, 14H), 7.37–7.31 (m, 4H), 7.18–7.16 (m, 2H), 2.11–2.01 (m, 12H), 1.30–1.08 (m, 72H), 0.90–0.71 (m, 18H).

### 7,7″-Dibromo-9,9,9′,9′,9″,9″-hexa-*n*-octyl-2,2′-7′,2″-terfluorene (6)

A solution of **5** (0.7 g, 0.6 mmol) in dichloromethane (1 mL) was added to a solution of bromine (0.25 g, 1.6 mmol) in dichloromethane (2 mL) and the mixture was refluxed with stirring for 1.5 h under an argon atmosphere. The mixture was poured into water and washed with sodium thiosulfate until the red color disappeared. The combined organic layer was dried over anhydrous $MgSO_4$ and concentrated *in vacuo* to give **6** as a pale yellow oil (0.8 g, 0.6 mmol, ca. 100%). $R_f$: 0.5 (for hexane).

$^1$H NMR (500 MHz, $CDCl_3$): $\delta$ (ppm) 8.00–7.35 (m, 18H), 2.05–1.95 (m, 12H), 1.25–1.09 (m, 72H), 0.85–0.81 (m, 18H).

### Poly[(9,9,9′,9′,9″,9″-hexa-*n*-octylfluorenyl-2,7′-diyl)-*alt*-4,4′-azobenzene)] (P3FAz)

*n*-BuLi in hexane (1.6 M, 2 mL) was added slowly to a stirred solution of **6** (0.8 g, 0.6 mmol) in THF (5 mL) at −78 °C under an argon atmosphere and the mixture was stirred for 1 h at −78 °C. Trimethyl borate (1.5 mL) was slowly added at −78 °C, and the mixture was then warmed slowly to room temperature and stirred continuous for 20 h. The mixture was then slowly cooled to 0 °C and then dilute hydrochloric acid (6 mL) was added. The mixture was extracted with diethyl ether and the resulting organic layer was dried over anhydrous $MgSO_4$. Concentration *in vacuo* gave the corresponding 9,9,9′,9′,9″,9″-hexa-*n*-octyl-7,2′-7′,7″-terfluorene-2,2″-diboronic acid (0.7 mg, 0.5 mmol). The resulting boronic compound (0.21 g, 0.17 mmol) was mixed with **1** (77 mg, 0.2 mmol) in toluene (3 mL) under a nitrogen atmosphere. This mixture was added to a solution of aqueous $K_2CO_3$ (2.0 M, 1.8 mL) and $Pd(PPh_3)_4(0)$ (3 mg) and stirred under reflux at 70 °C for 42 h. The mixture was poured into cold methanol and washed with dilute hydrochloric acid, and the polymer precipitate was collected on a filter. The polymer precipitate was resolved with toluene and poured into cold methanol three times. The polymer powder was collected by filtration to give **PF3Az** as an orange powder (86 mg, 0.07 mmol, 12%).

mp: 129–150 °C, decomposed at 277 °C. $M_w$: 21,000 g mol$^{-1}$, $M_w/M_n = 3.2$. $^1$H NMR (500 MHz, $CDCl_3$): $\delta$ (ppm) 7.90–7.72 (br), 2.16–2.13 (br), 1.22–1.00 (br). ATR-FTIR (cm$^{-1}$): 2923, 2849, 1599, 1465, 1230, 1220, 1156, 895, 819.

## RESULTS AND DISCUSSION

The poly(9,9-dioctylfluorene-*alt*-azobenzene)s (**PFAz**)s with different numbers of fluorene units and an azobenzene unit (**P1FAz**, **P2FAz**, and **P3FAz**) were synthesized by palladium-catalyzed Suzuki polymerization. A 0.2-$\mu$m diameter PTFE syringe filter was used to collect the monodisperse polymers. The syntheses were conducted according to procedures in the literature.[21–24] The procedure for synthesis of the **PFAz**s is shown in Scheme 1. The structures of the products were confirmed by MS, $^1$H NMR, and IR spectroscopy.

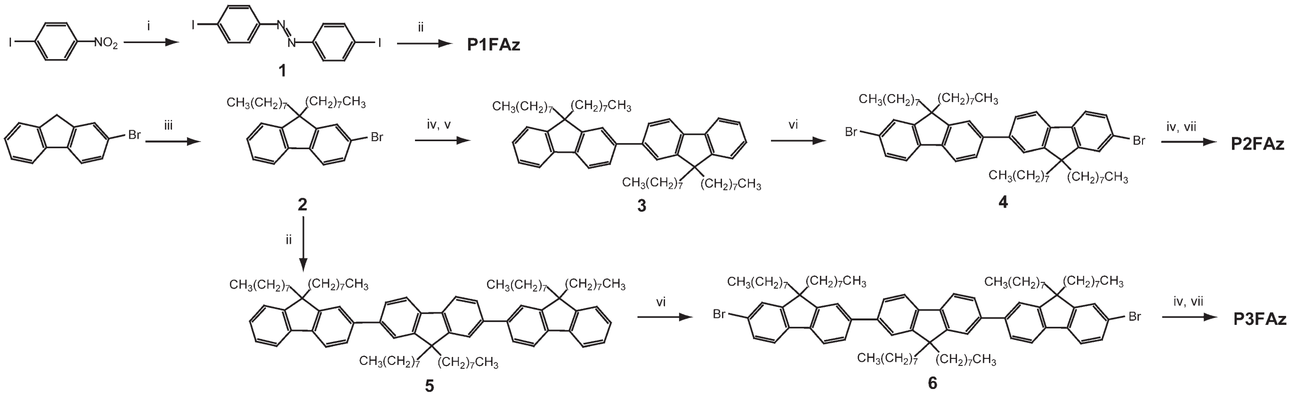

**SCHEME 1** Synthesis of poly(9,9-dioctylfluorene) copolymers: (i) Al, KOH, MeOH, rt; (ii) 9,9-dioctylfluorene-2,7-diboronic acid bis(1,3-propanediol)ester, $Pd(PPh_3)_4$, $K_2CO_3$, toluene, 70 °C; (iii) $CH_3(CH_2)_7Br$, DMSO, 50% NaOH aq., 35 °C; (iv) *n*-BuLi, $B(OMe)_3$, THF −78 °C; (v) $K_2CO_3$, $Pd(PPh_3)_4$, toluene, 75 °C; (vi) $Br_2$, $CH_2Cl_2$, reflux temperature; (vii) **1**, $K_2CO_3$, $Pd(PPh_3)_4$, toluene, 70 °C.

UV–vis absorption spectra of **PFAz**s in chloroform are shown in Figure 2(a–c). The **PFAz**s have a broad absorption that extends from 300 to 570 nm with a maxima at 417 nm for **P1FAz**, 390 nm for **P2FAz**, and 356 nm for **F3FAz**, respectively, which are attributed to the $\pi-\pi^*$ transitions of the fluorene backbone and azobenzene chromophore. In particular, the absorption bands appearing around 375–390 nm, which are clearly evident in the **P2FAz** and **P3FAz** spectra, are attributed to the $\pi-\pi^*$ transition of the conjugated polyfluorene backbone,[25,26] whereas the absorption bands greater than 400 nm shown in **P1FAz** are due to the $\pi-\pi^*$ transition of the azobenzene chromophore. This indicates that the copolymers do not have extended conjugation along the polymer main-chain; therefore, the conjugation could be twisted, due to steric hindrance around the 9-position dioctyl substituent in the fluorene unit, which prevents a system with fluorene-to-fluorene conjugation. The intensity of this UV−vis absorption band decreases for the **PFAz**s under 400 nm light irradiation [Fig. 2(a–c), dotted lines]. Simultaneously, the absorption bands at 500–550 nm increase slightly [inset in Fig. 2(a–c)], which indicate the *trans-cis* photoisomerization of the azobenzene moiety in the copolymers. The increase in these absorption bands is related to the absorption of the *cis*-isomer of azobenzene.[27,28] The initial intensities of the short-wave absorption band recover after exposure to visible light or spontaneous relaxation in the dark. After irradiation with 400 nm light, the differences in the absorption intensities of the **PFAz**s are dependent on the respective fluorine structures. The fluorescence spectra of **PFAz**s in chloroform were also measured; however, the intensity of all fluorescence spectra was extremely weak (data not shown). It is likely that intramolecular energy transfer from the photoexcited fluorine units to the azobenzene chromophore could occur, which would result in quenched fluorescence. Fluorescence quantum yield measurements produced extremely small $\Phi_f$ values: $6.7 \times 10^{-4}$ (**P1FAz**), $7.9 \times 10^{-4}$ (**P2FAz**), and about 0 (**P3FAz**).

Figure 2(d–f) shows UV–vis absorption spectra for the spin-coated **PFAz** films before and after irradiation with 400 nm light. Spectral features similar to those of the **PFAz**s in chloroform were observed before irradiation. Upon irradiation with 400 nm light, only the **P1FAz** film showed a decrease and slight increase in the intensity of the absorption band due to the *trans*-isomer [Fig. 2(d), dotted lines] and *cis*-isomer, respectively [inset in Fig. 2(d)]. The spectral changes of the **P1FAz** film slowly recovered to the initial state in the dark. For the **P2FAz** and **P3FAz** films, the occurrence of *trans-cis* photoisomerization did not contribute to spectral changes at 500–550 nm, which indicates that the **P2FAz** and **P3FAz** films are less light sensitive. The decreases of absorbance at 400 nm for the **P2FAz** as well as that for the **P3FAz** are attributed to photodecomposition of the azobenzene chromophore. The intense decreases did not recover to the initial state in the dark. The *trans-cis* photoisomerization rates of azobenzene chromophores tend to be strongly dependent on the matrix environment.[29–32] Therefore, the efficient light sensitivity of the **P1FAz** film suggests that the process of *trans-cis* photoisomerization is strongly dependent on the mobility of photosensitive azobenzene moieties in the polymer main-chain and on the glass-transition temperature. Thus, the most efficient *trans-cis* photoisomerization was for the **P1FAz** film, because the fluorene and azobenzene units are alternately bonded in the periodic polymer, which provides the polymer main-chain with flexibility. The fluorescence characteristics of the **PFAz** films could not be clearly detected, as for the chloroform solutions of the **PFAz**s. This fluorescence behavior had been reported from research on azobenzene liquid crystalline polymers, where the light energy absorbed during alignment changes both the molecular potential energy and the heat energy.[33]

Figure 3 shows the angular dependence of absorbance ($\lambda_{max} = 430$ nm) for the **P1FAz** film. Absorbance was measured after irradiation with linear polarized 400 nm light under annealing at 60 °C for 2 h, where 0° and 90° are the absorbance parallel to and perpendicular to the direction of the polarized light, respectively. The annealing temperature of 60 °C used in this work was determined from a study of the dichroic ratio dependence on the temperature (Fig. 4).The

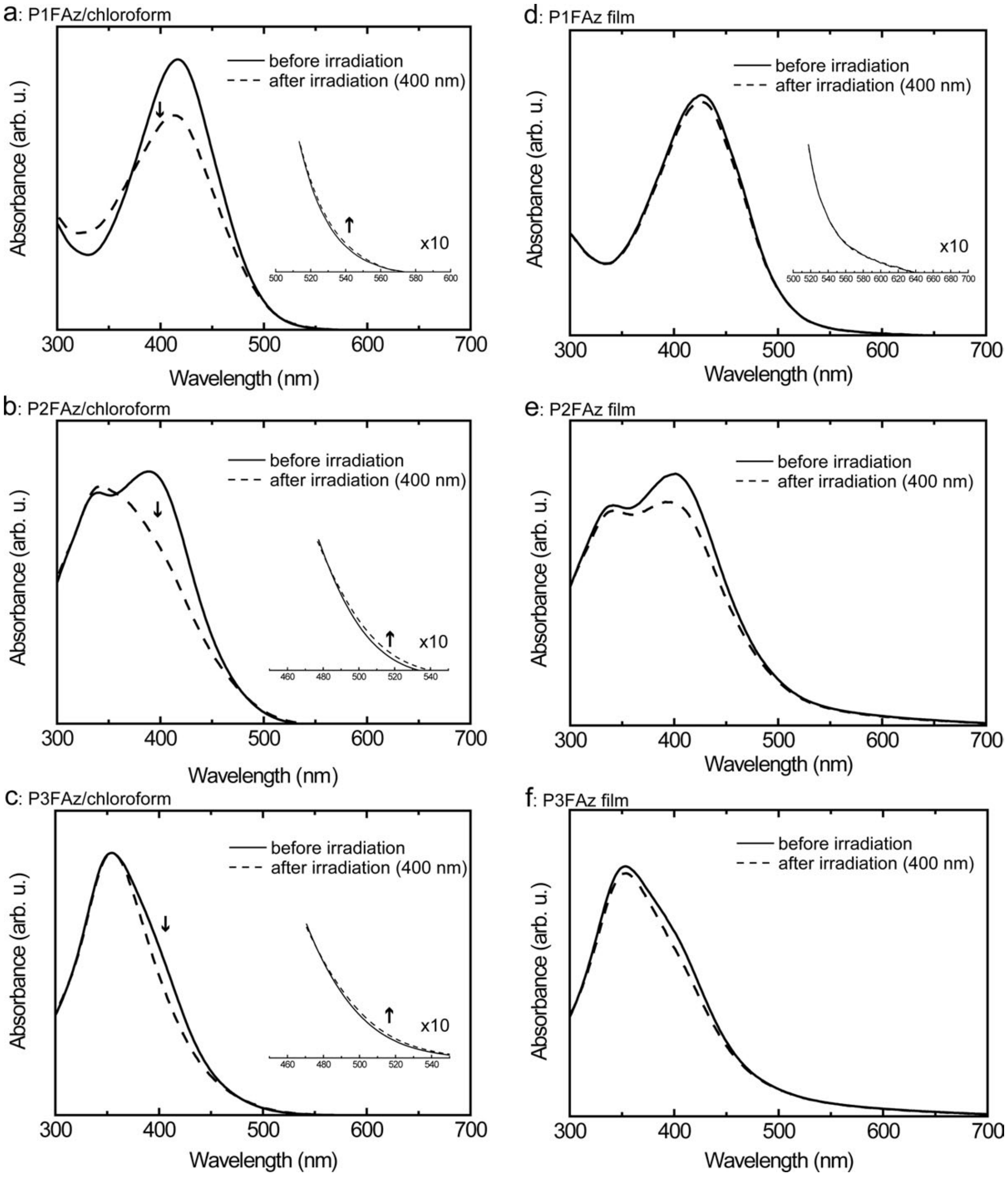

**FIGURE 2** UV–vis absorption spectra before and after irradiation with 400 nm light for (a) **P1FAz**, (b) **P2FAz**, (c) **P3FAz** in chloroform, and (d) **P1FAz**, (e) **P2FAz**, (f) **P3FAz** films. The insets show the respective spectra in more detail.

as-spun (before polarized light irradiation) **P1FAz** film shows no angular dependence and similar spectral features to the aforementioned spin-coated film—the orientational state of **P1FAz** film remains optically isotropic. Upon irradiation with linear polarized 400 nm light, the absorbance at 90° exhibits higher intensity compared to that at 0°, which results in a high dichroic ratio of 5.3. (The dichroic ratio is $A90^\circ/A0^\circ$ where $A90^\circ$ is the absorbance with respect to light polarized perpendicularly to the polarizing plane and $A0^\circ$ is the absorbance with respect to light polarized parallel to the polarizing plane.) For the last few decades, three principal processes have been proposed to induce anisotropy: angular hole burning, angular redistribution, and the rotational Brownian diffusion of the molecules.[34–36] According to the angular redistribution process, the azobenzene chromophore accumulates in a direction with the transition dipole axis perpendicular to the light polarization to minimize the absorption. Therefore, the result of angular dependency indicates that the polymer backbone of **P1FAz** involves the azobenzene unit aligned perpendicularly to the electric field vector of

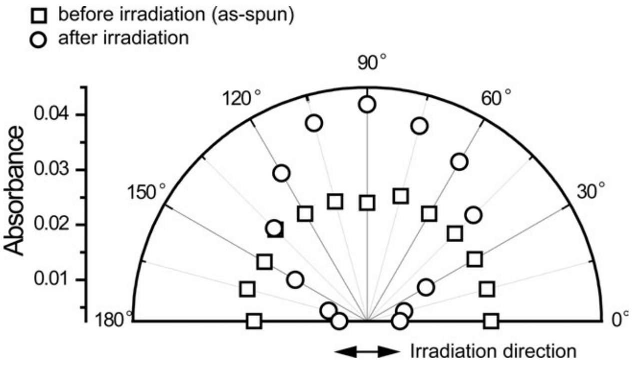

**FIGURE 3** Angular dependence of the absorbance for the **P1FAz** film (□) before polarized light irradiation and (○) after polarized light irradiation.

polarized light, and photo-induced alignment can be achieved during the repeated *trans*-to-*cis*-to-*trans*-... photoisomerization. To characterize the surface morphological effect of photo-induced alignment, the **P1FAz** film was observed by AFM (data not shown). However, no significant morphological changes were obtained and the root mean square (RMS) roughness was extremely small at 2−3 nm. AFM observation showed characteristics similar to those previously reported.[37] The results can also be explained briefly as follows. The polymer backbone is aligned perpendicularly to the electric field vector of polarized light after irradiation with linear polarized 400 nm light and is eventually crystallized in an extremely small area, thereby yielding a photo-alignment film. Thus, an as-spun **P1FAz** film surface could be assigned amorphous with random orientation.

The photo-induced alignment layer of the **P1FAz** film was applied to a poly(9,9-didodecylfluorene) (**F12**, $M_w$: 30,000 g mol$^{-1}$, $M_w/M_n = 2.0$) spin-coated film. The **F12** film was spin-coated on top of the photo-induced alignment layer of the **P1FAz** film from appropriate solutions. As the solvent for the surface oriented film cannot dissolve **P1FAz**, no significant intermixing of the two polymers is required. Thus, hexane was considered to be the most suitable solvent in this system. A surface oriented film on the photo-induced alignment layer of the **P1FAz** film was obtained by spin-coating of a 0.025 wt % hexane solution of **F12**, with subsequent annealing at 90 °C for 20 min followed by quenching (hereinafter referred to as "**F12/P1FAz** film"). The RMS roughness of the **F12/P1FAz** film was 1−2 nm. Figure 5 shows polarized absorption spectra of the **F12/P1FAz** film, where 0° and 90° are the absorption and fluorescence spectra parallel to and perpendicular to the direction of the polarized 400 nm light, respectively. The **F12/P1FAz** film has a broad absorption peak centered at 398 nm, which is attributed to the **F12** and **P1FAz** layers. The absorption spectra have a strong peak for 90° and a weak peak for 0°. The dichroic ratio of the **F12/P1FAz** film is estimated to be 2.1 from the ratio of absorption intensities. The resulting dichroic ratio indicates that the **F12** film has parallel orientation to the **P1FAz** film. Note that the polarized fluorescence spectra of the **F12/P1FAz** film, also shown in Figure 5, have a similar tendency to the absorption spectra characteristics. The dichroic ratio, estimated from the peak tops at 435 nm in the fluorescence spectra, was 1.6. Accordingly, orientation of the **F12** film was achieved by a combination of photochemical- and thermal-based processes. The most important feature of the surface orientation technique using the photo-induced alignment layer of the **P1FAz** film is that the arrangement of other polymers can be controlled, which would be useful for the fabrication of optoelectronics devices.

A schematic illustration of the overall technique presented here is summarized in Figure 6 and is described as follows: (i) Initial state: the surfaces of all polymer films have random ordering and the most stable conformation, the *trans*-isomer. (ii) Photoisomerization: upon irradiation with 400 nm light, the reversible *trans-cis* photoisomerization occurs only for the **P1FAz** film, and the polymer backbone of **P1FAz** aligns randomly. (iii) Photo-induced alignment: irradiation

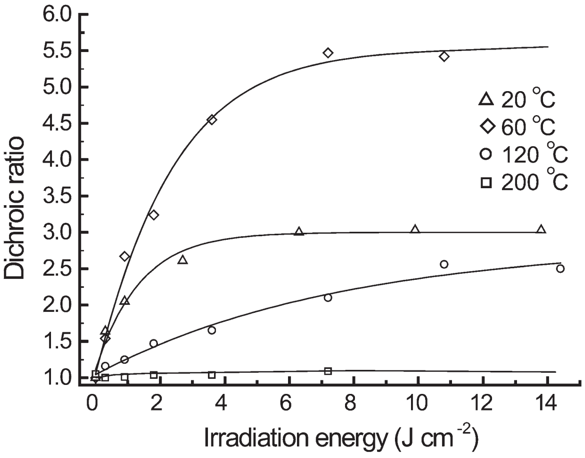

**FIGURE 4** Dichroic ratios of the **P1FAz** film as a function of irradiation energy.

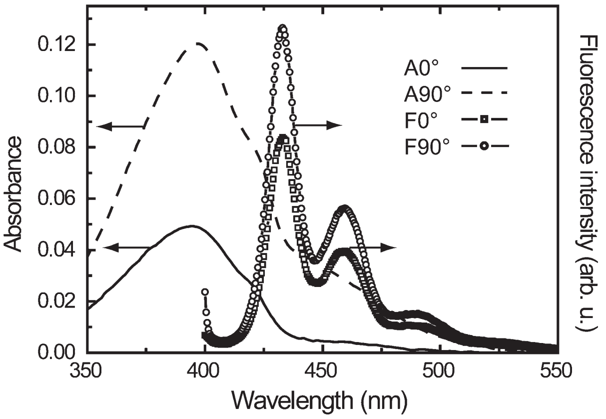

**FIGURE 5** Polarized UV–vis absorption spectra of the **F12/P1FAz** film after annealing at 90 °C for 20 min. *A*0° and *A*90° donate absorption parallel and perpendicular to the direction of polarized light, respectively. *F*0° and *F*90° denote fluorescence intensity parallel and perpendicular to the direction of polarized light, respectively.

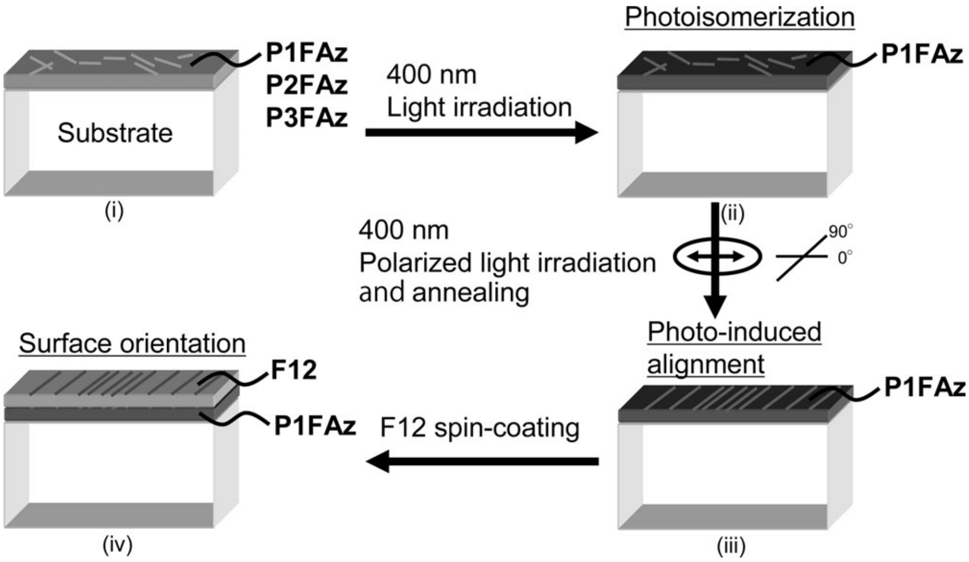

**FIGURE 6** Schematic representation of the overall mechanism for the surface orientation of **PFAz** films.

with polarized 400 nm light under annealing at 60 °C results in an accumulation of *trans*-isomers oriented perpendicular to the direction of polarized light for the **P1FAz** film after repeated periodic *trans-cis* photoisomerization. (iv) Surface orientation: the spin-coated **F12** film aligns parallel to the direction of the photo-induced alignment layer of the **P1FAz** film.

## CONCLUSIONS

Three types of bi-functionalized copolymers (**PFAz**) with azobenzene and fluorene units were successfully synthesized and characterized by UV–vis absorption and polarized absorption spectroanalysis. All synthesized polymers exhibited the *trans-cis* photoisomerization in chloroform. For the films, the occurrence of *trans-cis* photoisomerization and photo-induced alignment were observed only for the **P1FAz** film. Photo-induced alignment capability based on *trans-cis* photoisomerization was dependent on the number of fluorene units; therefore, the azobenzene functionalized polymer with fluorenes (two or more) showed no-photoisomerization capability even with annealing.

The *trans-cis* photoisomerization efficiency was dependent on the number of fluorene units, and photo-induced alignment was restricted by the orientation mobility of the azobenzene moieties, which has a strong influence to increase the main-chain rigidity of the copolymer backbone. Similarly, the decrease of fluorescence quantum yield corresponds directly to the increase of fluorene units, which suggests that the efficiency of intramolecular energy transfer to the azobenzene moieties is decreased with an increase in crystallinity with two and three fluorene units.

Surface orientation of an **F12** film was achieved using the photo-induced alignment layer of a **P1FAz** film and following annealing process. Thus, **P1FAz** will be useful for application as a photo-induced alignment material. These results will provide valuable information for the synthesis of azobenzene functionalized polymers and related structures in the design of optoelectronic devices.

## ACKNOWLEDGMENTS

This research was funded by a Grant-in-Aid for Challenging Exploratory Research (No. 23655186) from the Ministry of Education, Culture, Sports, Science and Technology of Japan.

## REFERENCES AND NOTES

**1** Matsunobe, T.; Nagai, N.; Kamoto, R.; Nakagawa, Y.; Ishida, H. *J. Photopolym. Sci. Technol.* **1995,** *8*, 263–268.

**2** Nishikawa, M. *Polym. Adv. Technol.* **2000,** *11*, 404–412.

**3** Gibbons, W. M.; Shannon, P. J.; Sun, S.-T. *Mol. Cryst. Liq. Cryst.* **1994,** *251*, 191–208.

**4** Ichimura, K.; Suzuki, Y.; Seki, T.; Hosoki, A.; Aoki, K. *Langmuir* **1988,** *4*, 1214–1216.

**5** Wiesner, U.; Reynolds, N.; Boeffel, C.; Spiess, H. W. *Makromol. Chem. Rapid Commun.* **1991,** *12*, 457–464.

**6** Wiesner, U.; Reynolds, N.; Boeffel, C.; Spiess, H. W. *Liq. Cryst.* **1992,** *11*, 251–267.

**7** Makita, Y.; Natsui, T.; Kimura, S.; Nakata, S.; Kimura, M.; Matsuki, Y.; Takeuchi, Y. *J. Photopolym. Sci. Technol.* **1998,** *11*, 187–192.

**8** Obi, M.; Morino, S.; Ichimura, K. *Chem. Mater.* **1999,** *11*, 1293–1301.

**9** Schadt, M.; Schmitt, K.; Kozinov, V.; Chigrinov, V. *Jpn. J. Appl. Phys.* **1992,** *31*, 2155–2164.

**10** Song, S.; Watabe, M.; Adachi, T.; Kobae, T.; Chen, Y.; Kawabata, M.; Ishida, Y.; Takahara, S.; Yamaoka, T. *Jpn. J. Appl. Phys.* **1998,** *37*, 2620–2624.

**11** Kawatsuki, N.; Takatsuka, H.; Kawakami, Y.; Yamamoto, Y. *Polym. Adv. Technol.* **1999,** *10*, 429–433.

**12** Schadt, M.; Seiberle, H.; Schuster, A.; Kelly, S. M. *Jpn. J. Appl. Phys.* **1995,** *34*, 3240–3249.

**13** Wu, Y. L.; Demachi, Y.; Tsutsumi, O.; Kanazawa, A.; Shiono, T.; Ikeda, T. *Macromolecules* **1998,** *31*, 4457–4463.

**14** Eich, M.; Wendorff, J. H.; Reck, B.; Ringsdorf, H. *Makromol. Chem. Rapid Commun.* **1987,** *8*, 59–63.

**15** Eich, M.; Wendorff, J. H.; Reck, B.; Ringsdorf, H. *Makromol. Chem. Rapid Commun.* **1987,** *8*, 457–460.

**16** Kinashi, K.; Ueda, Y. *Mol. Cryst. Liq. Cryst.* **2006,** *445*, 223–230.

**17** Sévigny, S.; Bouchard, L.; Motallebi, S.; Zhao, Y. *Macromolecules* **2003,** *36*, 9033–9041.

**18** Leclair, S.; Mathew, L.; Giguere, M.; Motallebi, S.; Zhao, Y. *Macromolecules* **2003,** *36*, 9024–9032.

**19** Misaki, M.; Ueda, Y.; Nagamatsu, S.; Yoshida, Y.; Tanigaki, N.; Yase, K. *Macromolecules* **2004,** *37*, 6926–6931.

**20** Sakamoto, K.; Miki, K.; Misaki, M.; Sakaguchi, K.; Hijikata, Y.; Chikamatsu, M.; Azumi, R. *J. Appl. Phys.* **2010,** *107*, 113108.

**21** Kreger, K.; Wolfer, P.; Audorff, H.; Kador, L.; Stingelin-Stutzmann, N.; Smith, P.; Schmidt H.-W. *J. Am. Chem. Soc.* **2010,** *132*, 509–516.

**22** Kageyama, Y.; Murata, S. *J. Org. Chem.* **2005,** *70*, 3140–3147.

**23** Wei, W.; Tomohiro, T.; Kodaka, M.; Okuno, H. *J. Org. Chem.* **2000,** *65*, 8979–8987.

**24** Ding, J.; Day, M.; Robertson, G.; Roovers, J. *Macromolecules* **2002,** *35*, 3474–3483.

**25** Yang, C.; Song, H.-S.; Liu, D.-B. *J. Mater. Sci.* **2012,** *47*, 3315–3319.

**26** Scherf, U.; List, E. M. J. *Adv. Mater.* **2002,** *14*, 477–487.

**27** Kamruzzaman, M.; Kuwahara, Y.; Ogata, T.; Ujiie, S.; Kurihara, S. *Polym. Int.* **2011,** *60*, 730–737.

**28** Kamruzzaman, M.; Kuwahara, Y.; Ogata, T.; Ujiie, S.; Kurihara, S. *J. Appl. Polym. Sci.* **2011,** *120*, 950–959.

**29** Haro, M.; Gascón, I.; Aroca, R.; López, M. C.; Royo, F. M. *J. Colloid Interface Sci.* **2008,** *319*, 277–286.

**30** Tamada, K.; Akiyama, H.; Wei, T. X. *Langmuir* **2002,** *18*, 5239–5246.

**31** Nakagawa, M.; Watase, R.; Ichimura, K. *Mol. Cryst. Liq. Cryst.* **2000,** *344*, 113–118.

**32** Fang, G.; Koral, N.; Zhu, C.; Yi, Y.; Glaser, M. A.; Maclennan, J. E.; Clark, N. A. *Langmuir* **2011,** *27*, 3336–3342.

**33** Zhao, D.; Zhang, Q.; Lu, Y.; Li, J.; Liu, J.; Cheng, X. *Macromol. Theory Simul.* **2003,** *12*, 690–695.

**34** Pedersen, T. G.; Johansen, P. M. *Phys. Rev. Lett.* **1997,** *79*, 2470–2473.

**35** Pedersen, T. G.; Johansen, P. M.; Holme, N. C. R.; Ramanujam, P. S.; Hvilsted, S. *J. Opt. Soc. Am. B* **1998,** *15*, 1120–1129.

**36** Delaire, J. A.; Nakatani, K. *Chem. Rev.* **2000,** *100*, 1817–1846.

**37** Koshiba, Y.; Yamamoto, M.; Kinashi, K.; Misaki, M.; Ishida, K.; Oguchi, Y.; Ueda, Y. *Thin Solid Films* **2009,** *518*, 805–809.